TOXICOLOGICAL SCIENCES **131(2)**, 375–386 2013
doi:10.1093/toxsci/kfs303
Advance Access publication October 22, 2012

Identification of *Dlk1-Dio3* Imprinted Gene Cluster Noncoding RNAs as Novel Candidate Biomarkers for Liver Tumor Promotion

Harri Lempiäinen,* Philippe Couttet,* Federico Bolognani,* Arne Müller,† Valérie Dubost,* Raphaëlle Luisier,* Alberto Del Rio Espinola,* Veronique Vitry,* Elif B. Unterberger,‡ John P. Thomson,§ Fridolin Treindl,¶ Ute Metzger,¶ Clemens Wrzodek,‖ Florian Hahne,† Tulipan Zollinger,* Sarah Brasa,* Magdalena Kalteis,* Magali Marcellin,* Fanny Giudicelli,* Albert Braeuning,‡ Laurent Morawiec,* Natasa Zamurovic,* Ulrich Längle,‖‖ Nico Scheer,‖‖ Dirk Schübeler,# Jay Goodman,** Salah-Dine Chibout,* Jennifer Marlowe,* Diethilde Theil,* David J. Heard,† Olivier Grenet,* Andreas Zell,‖ Markus F. Templin,¶ Richard R. Meehan,§ Roland C. Wolf, ††,[a] Clifford R. Elcombe,†† Michael Schwarz,‡ Pierre Moulin,* Rémi Terranova,*,[1] and Jonathan G. Moggs*,[1]

**Discovery and Investigative Safety and †Preclinical Safety Informatics, Preclinical Safety, Novartis Institutes for Biomedical Research, CH-4057 Basel, Switzerland; ‡Department of Toxicology, Institute of Experimental and Clinical Pharmacology and Toxicology, University of Tübingen, 72074 Tübingen, Germany; §Breakthrough Breast Cancer Research Unit and Division of Pathology, University of Edinburgh, Western General Hospital, Edinburgh EH4 2XU, UK; ¶NMI Natural and Medical Sciences Institute, University of Tübingen, 72770 Reutlingen, Germany; ‖Center for Bioinformatics Tübingen (ZBIT), University of Tübingen, 72074 Tübingen, Germany; ‖‖Department of Toxicology, Preclinical Safety, Novartis Institutes for Biomedical Research, CH-4057 Basel, Switzerland; ‖‖‖TaconicArtemis, Köln 51063, Germany; #Friedrich Miescher Institute for Biomedical Research, CH-4057 Basel, Switzerland; **Department of Pharmacology and Toxicology, Michigan State University, East Lansing, Michigan 48824; ††CXR Biosciences Ltd, Dundee DD1 5JJ, UK; and [a]Medical Research Institute, University of Dundee, Ninewells Hospital & Medical School, Dundee DD1 9SY, UK*

[1]To whom correspondence should be addressed at Discovery and Investigative Safety, Preclinical Safety, Novartis Institutes for Biomedical Research, CHBS WKL135, Klybeckstrasse 141, CH-4057 Basel, Switzerland. Fax: +41 61 3241027. E-mail: remi.terranova@novartis.com and jonathan.moggs@novartis.com

Received September 3, 2012; accepted October 12, 2012

The molecular events during nongenotoxic carcinogenesis and their temporal order are poorly understood but thought to include long-lasting perturbations of gene expression. Here, we have investigated the temporal sequence of molecular and pathological perturbations at early stages of phenobarbital (PB) mediated liver tumor promotion *in vivo*. Molecular profiling (mRNA, microRNA [miRNA], DNA methylation, and proteins) of mouse liver during 13 weeks of PB treatment revealed progressive increases in hepatic expression of long noncoding RNAs and miRNAs originating from the *Dlk1-Dio3* imprinted gene cluster, a locus that has recently been associated with stem cell pluripotency in mice and various neoplasms in humans. PB induction of the *Dlk1-Dio3* cluster noncoding RNA (ncRNA) *Meg3* was localized to glutamine synthetase-positive hypertrophic perivenous hepatocytes, suggesting a role for β-catenin signaling in the dysregulation of *Dlk1-Dio3* ncRNAs. The carcinogenic relevance of *Dlk1-Dio3* locus ncRNA induction was further supported by *in vivo* genetic dependence on constitutive androstane receptor and β-catenin pathways. Our data identify *Dlk1-Dio3* ncRNAs as novel candidate early biomarkers for mouse liver tumor promotion and provide new opportunities for assessing the carcinogenic potential of novel compounds.

Key Words: **nongenotoxic carcinogenesis; phenobarbital; biomarker; noncoding RNAs; Dlk1-Dio3 imprinted cluster; epigenetics.**

The initiating events leading to carcinogenesis are still poorly understood and may include temporal accumulation of genetic and epigenetic mutations associated with perturbed gene expression programs (Feinberg *et al.*, 2006; Jones and Baylin, 2007; Negrini *et al.*, 2010) leading to hallmark phenotypic alterations (Hanahan and Weinberg, 2011). Because tumor cells often display stem cell-like features, including reduced differentiation and increased proliferation, it has been suggested that tumors arise from the resident stem cell populations in tissues (Bonnet and Dick, 1997; Reya *et al.*, 2001). Alternatively, cancer cells may originate from differentiated postmitotic cells that have gained stem cell-like features by the sequential accumulation of mutations and clonal selection (Dyer and Bremner, 2005; Merlo *et al.*, 2006). The role of epigenetic mechanisms in the regulation of both carcinogenesis and cellular stemness is well established, and therefore it has been suggested that epigenetic changes might be among the first and initiating events during carcinogenesis (Feinberg *et al.*, 2006). Epigenetic mechanisms that may be deregulated in carcinogenesis include DNA methylation, histone posttranslational modifications, and noncoding RNAs (ncRNAs) (Berdasco and Esteller, 2010; Esteller and Rodriguez-Paredes, 2011; Prasanth and Spector, 2007). MicroRNAs (miRNAs) are the best-characterized regulatory ncRNAs. These small 20- to 22-nucleotide-long RNAs regulate the translation of their target messenger RNAs (mRNAs) by

targeting complementary antisense sequences in the transcripts (Bartel, 2004). Another interesting, but yet poorly understood, class of ncRNAs are the long noncoding RNAs (lncRNAs) (Chen and Carmichael, 2010), which are generally defined as over ~200-nucleotide-long RNAs without apparent coding functions. Known functions of lncRNAs are linked to the regulation of chromatin and nuclear structure both in *cis* and *trans* (Chen and Carmichael, 2010; Khalil *et al.*, 2009), and several lncRNAs play key roles in development, including the regulation of pluripotency, differentiation, and genomic imprinting (Koerner *et al.*, 2009; Guttman *et al.*, 2011).

Environmental factors such as nutrition or xenobiotics can trigger changes in gene expression programs to ensure appropriate adaptive responses to changing conditions. Exposure to xenobiotic toxicants, including several nongenotoxic carcinogens, can lead to profound and long-lasting, heritable epigenetic perturbations (Lebaron *et al.*, 2010; Lempiainen *et al.*, 2011; Koturbash *et al.*, 2011). The characterization of early transcriptional and epigenetic mechanisms during nongenotoxic carcinogenesis (NGC) is a promising approach for the identification of novel safety biomarkers.

Phenobarbital (PB) is an anticonvulsant commonly used for treatment of epilepsy and other seizures. In rodents, PB promotes both spontaneous and chemically induced liver tumors, with chronic treatment leading to a significant increase in hepatic tumor incidences (Becker, 1982). PB is the classic nongenotoxic rodent carcinogen (Whysner *et al.*, 1996) and has been used widely as a model compound for studying mechanisms underlying nongenotoxic chemical carcinogen-induced rodent liver carcinogenesis (Lempiainen *et al.*, 2011; Phillips *et al.* 2009a,b; Ross *et al.*, 2010; Yamamoto *et al.*, 2004). Liver tumor promotion by PB is dependent on constitutive androstane receptor (CAR) and β-catenin (Huang *et al.*, 2005; Rignall *et al.*, 2011; Yamamoto *et al.*, 2004), and prolonged PB treatment selects for *Ctnnb1* (encoding β-catenin) mutated tumors (Aydinlik *et al.*, 2001). PB regulates the nuclear localization of CAR, and CAR is required for PB-induced early gene expression changes and hyperplasia/hypertrophy (Kawamoto *et al.*, 1999; Phillips *et al.*, 2009a; Ross *et al.*, 2010). In addition to CAR, PB also activates another nuclear receptor, called pregnane X receptor (PXR) (Lehmann *et al.*, 1998), which has overlapping functions with CAR to regulate xenobiotic metabolism and detoxification in liver (Tolson and Wang, 2010). Several rodent studies have reported time- and tissue-specific gene expression and DNA methylation perturbations upon PB treatment, both at early stages of liver tumor promotion and in tumors (Bachman *et al.*, 2006; Counts *et al.*, 1996; Goodman and Watson, 2002; Kostka *et al.*, 2007; Lempiainen *et al.*, 2011; Phillips *et al.*, 2007; Phillips and Goodman, 2008; Phillips *et al.*, 2009a,b).

To investigate the temporal sequence of gene regulatory events underlying tumor promotion by a nongenotoxic carcinogen *in vivo*, we have used integrated molecular profiling of coding RNA and ncRNA species, DNA methylation, protein expression, and protein modifications anchored to histopathological analyses at seven time points (1 day to 13 weeks) in PB-treated and vehicle-treated B6C3F1 mice. We show that early PB-induced molecular responses include the progressive increase in hepatic expression of lncRNAs and miRNAs from the *Dlk1-Dio3* imprinted gene cluster. The carcinogenic relevance of *Dlk1-Dio3* lncRNAs is further supported by their genetic dependence on CAR and β-catenin, two pathways essential for PB-mediated liver tumor promotion. These novel ncRNA candidate early biomarkers may provide useful mechanism-of-action-based tools for the early detection and prediction of xenobiotic-induced nongenotoxic hepatocarcinogenesis.

MATERIALS AND METHODS

Ethics statement. *In vivo* rodent studies were performed following either University of Tübingen institutional guidelines (Rignall *et al.*, 2011) or in conformity with the Swiss Animal Welfare Law (specifically under the Animal Licenses No. 2345 by "Kantonales Veterinäramt Basel-Stadt" [Cantonal Veterinary Office, Basel] and No. 5041 by "Kantonales Veterinäramt Baselland" [Cantonal Veterinary Office, Basel Land]).

Animal treatment and sample preparation. For the seven-time point 13-week study, 29- to 32-day-old male B6C3F1/Crl (C57BL/6 ♀ × C3H/He ♂) mice were obtained from Charles River Laboratories (Germany). For the 13-week (+ 4-week recovery) study, 9- to 11-week-old CAR^{KO}/PXR^{KO} (Scheer *et al.*, 2008) and wild-type (WT) C57BL/6 male mice were obtained from Taconic (Germany). Animals were allowed to acclimatize for 5 days prior to being randomly divided into two treatment groups ($n = 5$ per time point). PB (Sigma [St Louis, MO] #04710, 0.05% [wt/vol] in drinking water) was administered to one group through *ad libitum* access to drinking water. Mice were checked daily for activity and behavior and sacrificed on the indicated dates. Blood was withdrawn for PK analysis, and liver was removed, split into several sections, either frozen in liquid nitrogen and stored at −80°C for subsequent analyses or fixed in neutral phosphate-buffered formalin, and embedded in paraffin wax. To ensure sample homogeneity for different molecular profiling methods, frozen liver samples were reduced to powder with Covaris Cryoprep (Covaris Inc., Woburn, MA) system and aliquoted on dry ice. The hepatocyte-specific knockout (KO) of β-catenin (*Ctnnb1*) in C3H/N background has been described recently (Rignall *et al.*, 2011). Starting at 8 weeks of age, WT and KO mice were either kept on a standard diet or on a diet containing 0.05% PB for 12 weeks prior sacrifice. Livers were excised; aliquots of liver were frozen on dry ice and stored at −80°C.

Affymetrix labeling, GeneChip processing, and gene expression data analysis. Affymetrix labeling, GeneChip processing, and gene expression data analysis were conducted as described in the Supplementary Materials and Methods. All the analyses were performed in R using Bioconductor packages (www.r-project.org/ and www.bioconductor.org) (Gentleman *et al.*, 2004) unless stated otherwise. Robust multiarray average (RMA) preprocessing was applied using the implementation of the algorithm available in R/Bioconductor (Irizarry *et al.*, 2003). Before statistical analysis, the data were filtered to remove low-expressed probe sets. Probe sets with log 2 raw intensity values below 6 in all groups were removed of the dataset. A two-way ANOVA model (treatment and time) was then fitted to the data to assess statistical significance and linear contrasts at each time point using the Bioconductor's Limma package, which uses a Bayesian approach to better estimate the variance (Smyth, 2005). The Benjamini-Hochberg method was applied to correct for multiple comparisons (Benjamini and Hochberg, 1995). Probe sets with p values lower than 0.01 and fold changes above 1.5 were considered differentially expressed. For cluster analysis, Euclidean distance was used as a similarity measure, and the Ward method of linkage was applied. For summarizing the fold changes of

specific clusters or probe set lists, the average fold change of each probe set in the list was calculated. For the comparison of the three studies in different strain backgrounds (B6C3F1, C57BL/6, and C3H) were normalized and analyzed together, using the same methods as above. Principal component analysis grouped the biological replicates together and separated different groups based on time point and treatment (Supplementary fig. S1A). The time-dependent separation of control groups was due to the young age (4–5 weeks old) of animals at beginning of the treatment and the strong time-dependent liver maturation effect in both control and PB-treated animals (data not shown). The liver maturation signal was subtracted (by comparing PB-treated samples with corresponding controls at each time point) from the downstream analyses reported here in order to focus only on PB treatment-associated transcriptional changes.

RNA isolation, RT-qPCR, and single-nucleotide polymorphism-sequencing analyses. RNA isolation and RT-qPCR analysis were conducted as described in the Supplementary Materials and Methods. Exonic single-nucleotide polymorphisms (SNPs) distinctive from C3H and C57BL/6 strains were identified from Mouse Genomes Project database (Wellcome Trust Sanger Institute; Keane *et al.*, 2011) and confirmed in the Mouse Genomic Database (Eppig *et al.*, 2012) for concordance. Selected polymorphisms were sequenced (forward and reverse) from C3H, C57BL/6, and B6C3F1 genomic DNA to confirm the appropriate genotypes (reported homozygous in the parental strains and heterozygous in B6C3F1), and confirmed SNPs were then evaluated on cDNA obtained from C3H, C57BL/6, and B6C3F1 treated or not with PB. In these experiments, RNA samples were treated with DNase to ensure the RNA purity and retrotranscribed with High Capacity kit. PCR products were purified with ExoSAP-IT (Affymetrix, OH). Sequencing reactions were performed with BigDye Terminator v3.1, purified with X-Terminator and run on an ABI 3730 DNA Analyzer (Life Technologies) following manufacturer procedures. Electropherograms were aligned using CLC Workbench 6 (CLC Bio, Aarhus, Denmark). Primers and PCR conditions available upon request.

miRNA low-density array analysis. miRNA profiling using TaqMan Array Rodent microRNA cards (Applied Biosystems/Life Technologies, Carlsbad, CA) was conducted as described in the Supplementary Materials and Methods.

hMeDIP and MeDIP protocols, array data processing, and analyses. HmeDIP and MeDIP experiments have been described in our earlier work (Thomson *et al.*, 2012). Normalization of the log 2 probe enrichments of the IP over input signals from the Nimblegen 2.1M deluxe mouse promoter (mm9 build) arrays was performed with the Bioconductor LIMMA package (Smyth, 2004) using median subtraction (within array) and scaling (between arrays), for visualization the normalized log 2 probe enrichments were median smoothed in a 600-bp sliding window (approximately six probes).

Reverse protein array. Reverse protein array (RPA) analysis on the ZeptoMARK assay platform (Bayer Technology Services, Leverkusen, Germany) was performed as described in the Supplementary Materials and Methods.

In situ *hybridization and immunohistochemistry.* *In situ* hybridization (ISH) and immunohistochemistry (IHC) analysis were conducted as described in the Supplementary Materials and Methods.

CAR/PXR binding site prediction at Dlk1-Dio3 cluster. Three CAR/PXR motif-PFMs were found in the Transfac Professional database (2011/Q3 release): VPXR_Q2, VDR4_Q2, and V$DR3_Q4. Motif matches were scanned within the *Dlk1-Dio3* locus (Chr12:110603831-111647695) with stringent filters (minFP, i.e., conservative, high cutoffs) minimizing the false positives (Wrzodek *et al.*, 2010).

RESULTS

Chronic PB Treatment Leads to Transient Hepatocyte Hyperplasia and Hepatocyte Hypertrophy

Chronic PB treatment results in 100% liver tumor incidence in B6C3F1 mice (Becker, 1982). However, the precise kinetics of molecular changes and their association with phenotypic changes in the liver have not been established. To address these questions, a kinetic study (1, 3, 7, 14, 28, 57, and 91 days of treatment) was run in B6C3F1 mice with *ad libitum* PB (0.05% [wt/vol] in drinking water) administration (Fig. 1A). Exposure analysis by liquid chromatography-mass spectrometry confirmed consistent PB plasma levels in all PB-treated animals (data not shown). The most striking histopathological abnormality detected was hepatocellular hypertrophy observed starting from 7 days of PB treatment and increasing in severity at later time points (Fig. 1B). Hypertrophy was primarily detected at perivenous hepatocytes in the central zone of the lobule (zone III) (Fig. 1C). Ki67 staining of the liver slides also revealed a transient mitotic response at earliest time points of PB treatment (Fig. 1C, bottom).

PB Treatment Causes Temporal Perturbations of the Transcriptome

To study early events of liver tumor promotion, the temporal sequence of transcriptional perturbations associated with PB-treatment was analyzed by microarray-based gene expression profiling. PB treatment affects the transcription of a large number of genes in the liver, with ~2000 genes significantly (> 1.5-fold change, adjusted p-value < 0.01) deregulated in at least one time point of the study (Supplementary fig. S1B and table S1). The largest number of transcriptional changes was detected after 1 day of PB treatment (Supplementary fig. S1B and table S1) attributable to transient upregulation of cell cycle/mitosis-related genes (Fig. 2 and Supplementary fig. S1B and table S2; cluster 8). Drug metabolism genes, including cytochrome P450 (e.g., *Cyp2b10*) family enzymes, were strongly upregulated already after 1 day of PB exposure, and their expression remained high throughout the 13-week study (Fig. 2, Supplementary figs. S1B and S2 and table S2; clusters 1, 3, 4, and 5). Cluster 3 contained several genes involved in cell cycle or stem cell regulation, including *Wisp1*, *Meig1*, *Gadd45b*, and *Prom1*, consistent with previous reports (Lempiainen *et al.*, 2011; Phillips *et al.*, 2009a,b). Among the genes downregulated by PB (Supplementary figs. S1B and S2 and table S2; clusters 6 and 7), no strong enrichment for specific biological processes could be detected. To complement the gene expression analyses and extend the analysis to posttranscriptional modifications, 159 proteins/protein PTMs were measured using reverse protein arrays (Hartmann *et al.*, 2009). The proteins/modifications were selected based on literature sand are involved in liver xenobiotic response/metabolism, liver tumor promotion, and growth regulation signaling pathways (full list in Supplementary table S3). Consistent with the transcription analysis, PB-induced changes in protein levels were observed for xenobiotic metabolism enzymes, including CYP450 enzymes and reductase POR (Supplementary figs. S3A and S3B and table S1), which were upregulated throughout the time course starting from day 1 of PB treatment. Other observed changes include perturbations in the components of the AMPK-, Aurora B-, and MEK-signaling pathways (Supplementary figs. S3A and S3B).

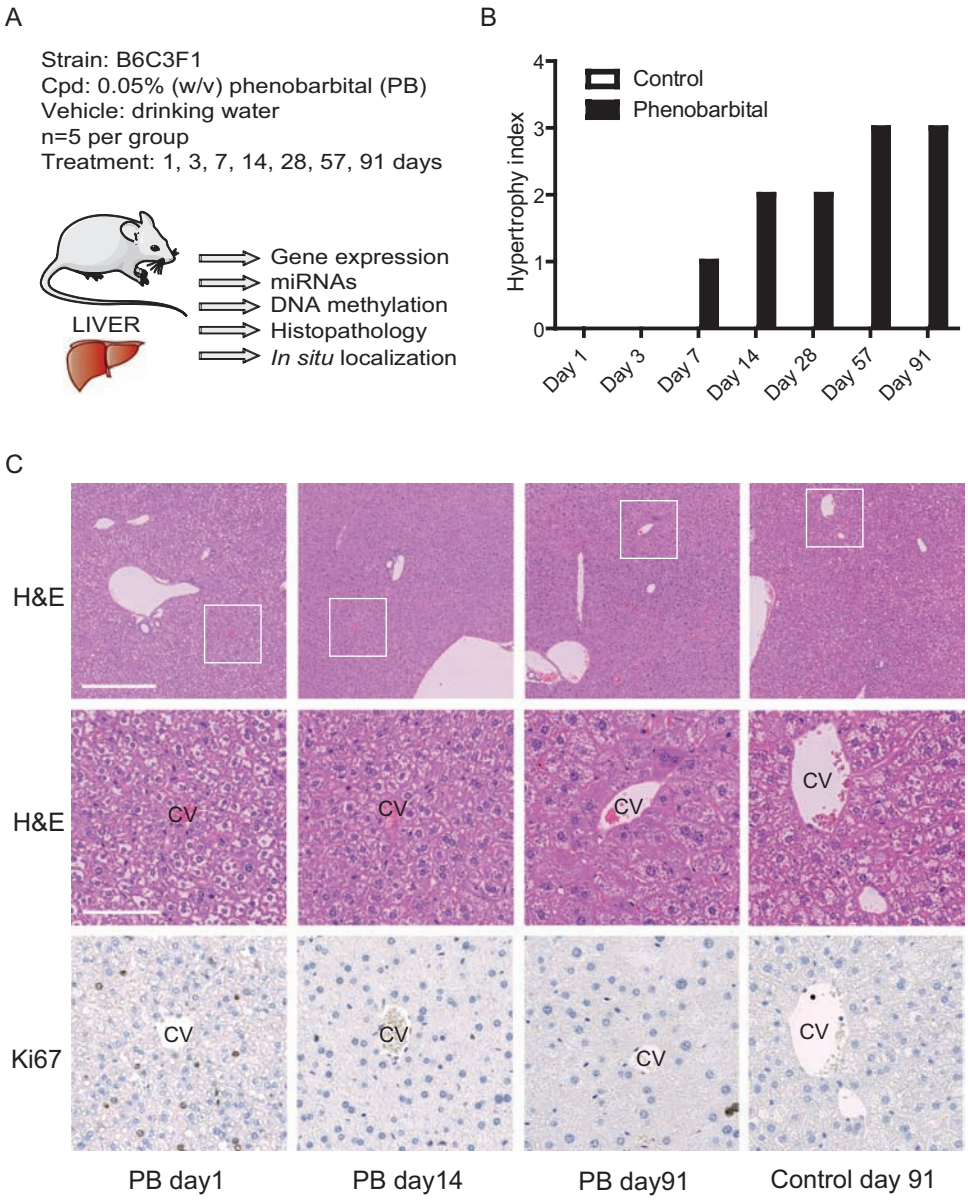

FIG. 1. Chronic PB treatment leads to hepatocyte hypertrophy. (**A**) Experimental design of the kinetic PB study for molecular and phenotypic profiling. Male B6C3F1 mice were given *ad libitum* access to PB or vehicle (drinking water). Mice were sacrificed at indicated time points; livers were sampled and aliquots used for genome-wide gene expression, miRNA, miRNA, DNA methylation (28-day time point only), chromatin posttranslation modifications (PTM; 28-day time point only), histopathology, and localization studies. (**B**) Hepatocellular hypertrophy index. Hepatocellular hypertrophy was evaluated by histopathology and H&E staining. The severity of hepatocellular hypertrophy was graded from 1 to 4. (**C**) Histopathology of the liver from PB-treated animals. Upper panel shows low-magnification encompassing central and portal areas (bar = 400 µm). Middle panel shows higher magnification of boxed centrilobular areas (boxed) from upper panel (bar = 100 µm). Bottom panel shows Ki67 immunoreactivity in areas corresponding to middle panel. Central vein is indicated by "CV."

Temporal Accumulation of Dlk1-Dio3 Cluster ncRNAs Upon PB Treatment

To investigate the potential role of miRNA perturbations in early tumor promotion, we performed an miRNome analysis for all the time points of the kinetic PB study. The expression of 784 miRNAs was measured from the liver samples of each animal of the study using ABI TaqMan miRNA low-density arrays (LDA). Forty-three miRNAs were significantly (greater than twofold change, adjusted p-value < 0.05) regulated by PB (Fig. 3A and Supplementary table S4), many of which were induced by PB from day 7 onwards with levels increasing at later time points (Fig. 3A). Strikingly, the majority (38) of the induced miRNAs are transcribed from the *Dlk1-Dio3* imprinted genomic cluster on chromosome 12qF1 (Fig. 3B). Several ncRNAs can be transcribed from the *Dlk1-Dio3* cluster, including ~50 miRNAs, a large group of snoRNAs and several

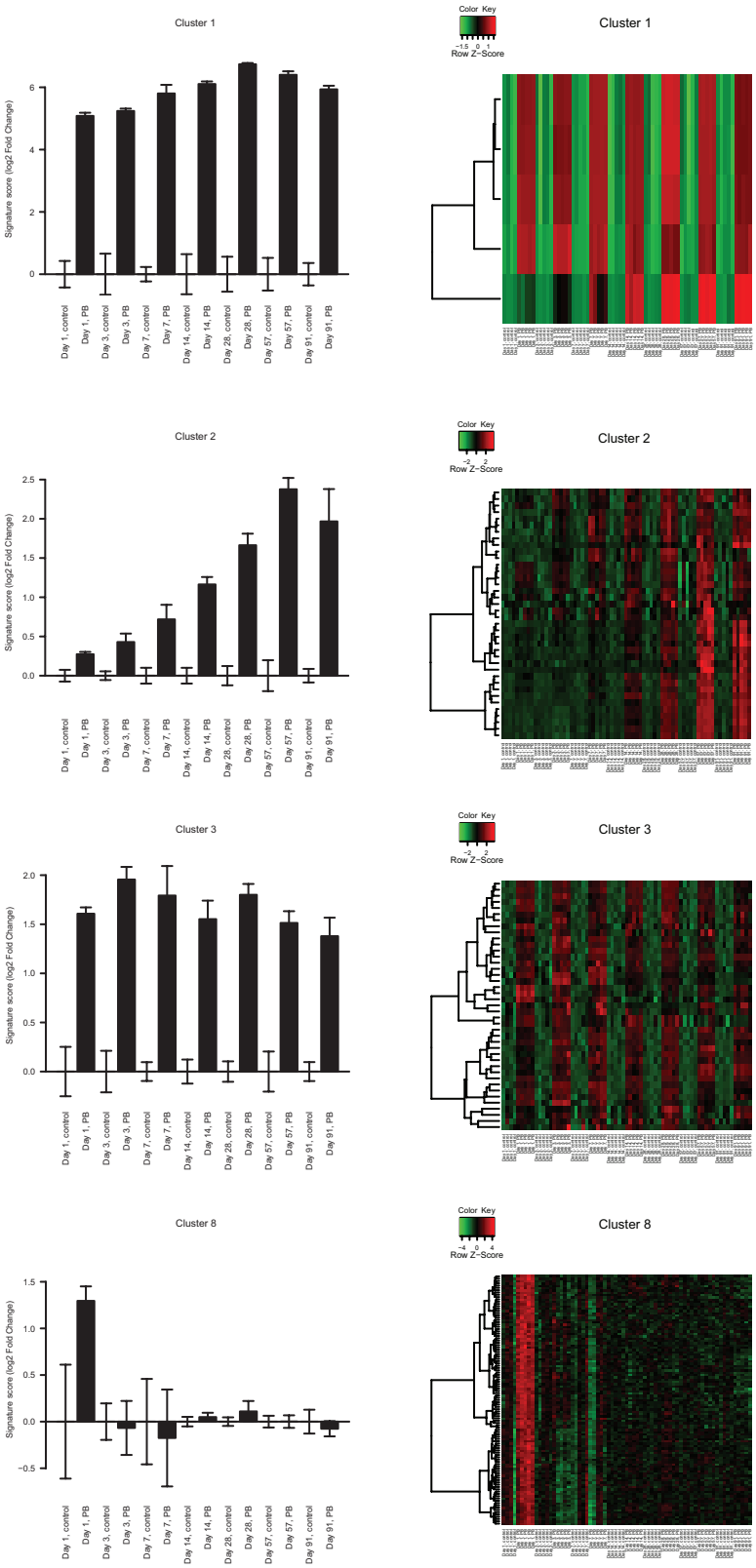

FIG. 2. PB treatment causes dynamic perturbations in the liver transcriptome. Signature score (log 2 fold changes) (left panel) and heat maps (middle panel) for selected gene expression clusters are shown. Gene expression clusters were generated using hierarchical clustering on RMA values of Affymetrix GeneChips probes that were significantly (> 1.5-fold change, p-value < 0.01) affected by PB treatment. Representative genes from each cluster are listed (right panel). For the full data set, see Supplementary figures S1 and S2 and table S1.

lncRNAs (Fig. 3B) and deregulation of a single large noncoding precursor RNA may account for these observations (Xie *et al.*, 2012). Consistent with the upregulation of most miRNAs from the *Dlk1-Dio3* cluster, the lncRNAs *Meg3* and *Rian* were upregulated starting from day 7 of PB treatment (Fig. 2 and Supplementary fig. S1 and table S2; cluster 2).

Due to the genomic imprinting, under normal conditions, the ncRNAs are expressed only from the maternally inherited *Dlk1-Dio3* cluster allele, whereas the three protein-coding mRNAs (*Dlk1*, *Rtl1*, and *Dio3*) are expressed from the paternally inherited allele. The PB induction of *Meg3* and *Rian* lncRNAs at the 28-day time point of the study was confirmed by RT-qPCR (Fig. 3C). *Mirg* lncRNA and *Rtl1* transcripts were also upregulated upon PB exposure (Fig. 3C and Supplementary table S1), whereas the expression of the two protein-coding genes flanking the region (i.e., *Dlk1* and *Dio3*; Fig. 3B) was unaffected (Fig. 3C). To investigate the allelic origin of *Dlk1-Dio3* lncRNAs induction, we sequenced genomic DNA and cDNA from parental strains (B6C3F1 originates from a cross between female C57BL/6 and male C3H) to identify parental specific polymorphisms (Supplementary fig. S4A) that can be used to discriminate allelic origin of *Dlk1-Dio3* induction. These analyses identified a series of SNPs within different regions of the imprinted cluster (Supplementary fig. S4A) and demonstrated that the lncRNAs are transcribed and induced by PB from the maternal allele (Fig. 3D and Supplementary fig. S4A). These analyses were also confirmed using SYBR Green qPCR assays with strand-specific primers to demonstrate that PB induces transcription of *anti-Rtl1* (maternal), but not *Rtl1* (Supplementary fig. S4B). In summary, these allelic analyses show induction of the lncRNAs from the maternal allele, suggesting increased expression from the maternal allele rather than loss of imprinting. The lack of any striking DNA methylation changes upon PB treatment (Supplementary fig. S5; Thomson *et al.*, 2012) at the *Meg3* promoter and intergenic imprinting regulatory regions (Sato *et al.*, 2011) is consistent with imprinting of the locus not being affected. The upregulation of *Dlk1-Dio3* cluster ncRNAs might involve direct transactivation by nuclear receptors such as CAR/PXR via one or more of ~25 putative CAR/PXR-binding sites (Supplementary table S5).

PB Induces Meg3 Expression in Glutamine Synthetase-Positive Hypertrophic Hepatocytes

To further investigate the possible role of the *Dlk1-Dio3* cluster ncRNAs in early pathological events of NGC, we used the molecular localization of *Meg3* lncRNA expression as a representative surrogate marker for determining the liver cell-type specificity of *Dlk1-Dio3* cluster ncRNA expression and modulation by PB. ISH using DIG-labeled single-stranded riboprobes targeting a conserved 500-bp region in the *Meg3* transcript was used to localize *Meg3* in liver sections. Very few cells expressed *Meg3* in untreated liver or at early time points of PB treatment (Fig. 4) consistent with *Meg3* transcript profiling data from homogenized liver tissue (Fig. 2; cluster 2). An increased number of cells expressing *Meg3* were detected after 14 days of PB treatment and continued to increase with time (Fig. 4). The *Meg3* transcript is detected in the nuclei of perivenous hepatocytes in the central zone of the lobule and the hepatocytes expressing *Meg3* are hypertrophic, suggesting that expression of *Dlk1-Dio3* cluster ncRNAs may be linked to hypertrophic phenotype.

Tumor promotion by PB is also dependent on the β-catenin signaling pathway (Rignall *et al.*, 2011), and PB-promoted tumors often have activating mutations in the *Ctnnb1* gene (Aydinlik *et al.*, 2001). Glutamine synthetase (GS) expression is directly regulated by β-catenin, and GS can be used as marker for *Ctnnb1*-mutated tumors (Loeppen *et al.*, 2002). To test if β-catenin signaling may be involved in the dysregulation of *Dlk1-Dio3* cluster ncRNAs upon PB exposure colocalization of *Meg3* (ISH) and GS (IHC) was assessed (Fig. 4). *Meg3* expression was almost exclusively detected in GS-positive cells (~90% colocalization), supporting a link between β-catenin signaling and *Meg3* expression.

CAR and β-Catenin Signaling Regulate Dlk1-Dio3 Cluster Expression

To investigate the mechanistic basis of PB-mediated perturbations in *Dlk1-Dio3* cluster ncRNA expression, we assessed potential genetic dependence on CAR and β-catenin pathways that have previously been shown to be essential for PB-mediated mouse hepatocarcinogenesis (Huang *et al.*, 2005; Rignall *et al.*, 2011; Yamamoto *et al.*, 2004). C57BL/6 CAR/PXR double KO (CAR^{KO}/PXR^{KO}) and WT mice (Scheer *et al.*, 2008) were treated for 13 weeks with PB (or vehicle). Maternally transcribed *Meg3* and *Rian* ncRNAs, but not paternally transcribed *Dlk1* mRNA, were upregulated by PB in C57BL/6 WT animals (Supplementary figs 5A and S6) consistent with our observations in B6C3F1 mice (Fig. 3). In contrast to B6C3F1 mice, no upregulation of *Mirg* was detected in the C57BL/6 animals (Supplementary fig. S6), which might be due to the very low microarray signal levels for *Mirg*. No PB-mediated induction of *Meg3* or *Rian* expression was observed in CAR^{KO}/PXR^{KO} mice indicating that CAR/PXR are required for the PB induction of the *Dlk1-Dio3* cluster ncRNAs. Transcript profiling of CAR KO C3H/He mice (Phillips *et al.*, 2009a) further supports CAR-mediated regulation of hepatic Meg3 transcription. We also assessed the reversibility of PB-induced genes 4 weeks after the removal of PB from the diet (following 13 weeks of PB exposure). Expression of the genes that were induced after 13-week PB exposure (*Meg3*, *Rian*, and *Cyp2b10*) returned back to basal levels after the 4-week recovery period (Fig. 5A), indicating that the PB effect on *Dlk1-Dio3* cluster and *Cyp2b10* expression was reversible.

The contribution of β-catenin signaling to the expression of *Dlk1-Dio3* cluster transcripts was evaluated using conditional hepatocyte-specific *Ctnnb1* KO mice ($Ctnnb1^{KO}$) and corresponding WT animals (in C3H background) (Rignall *et al.*,

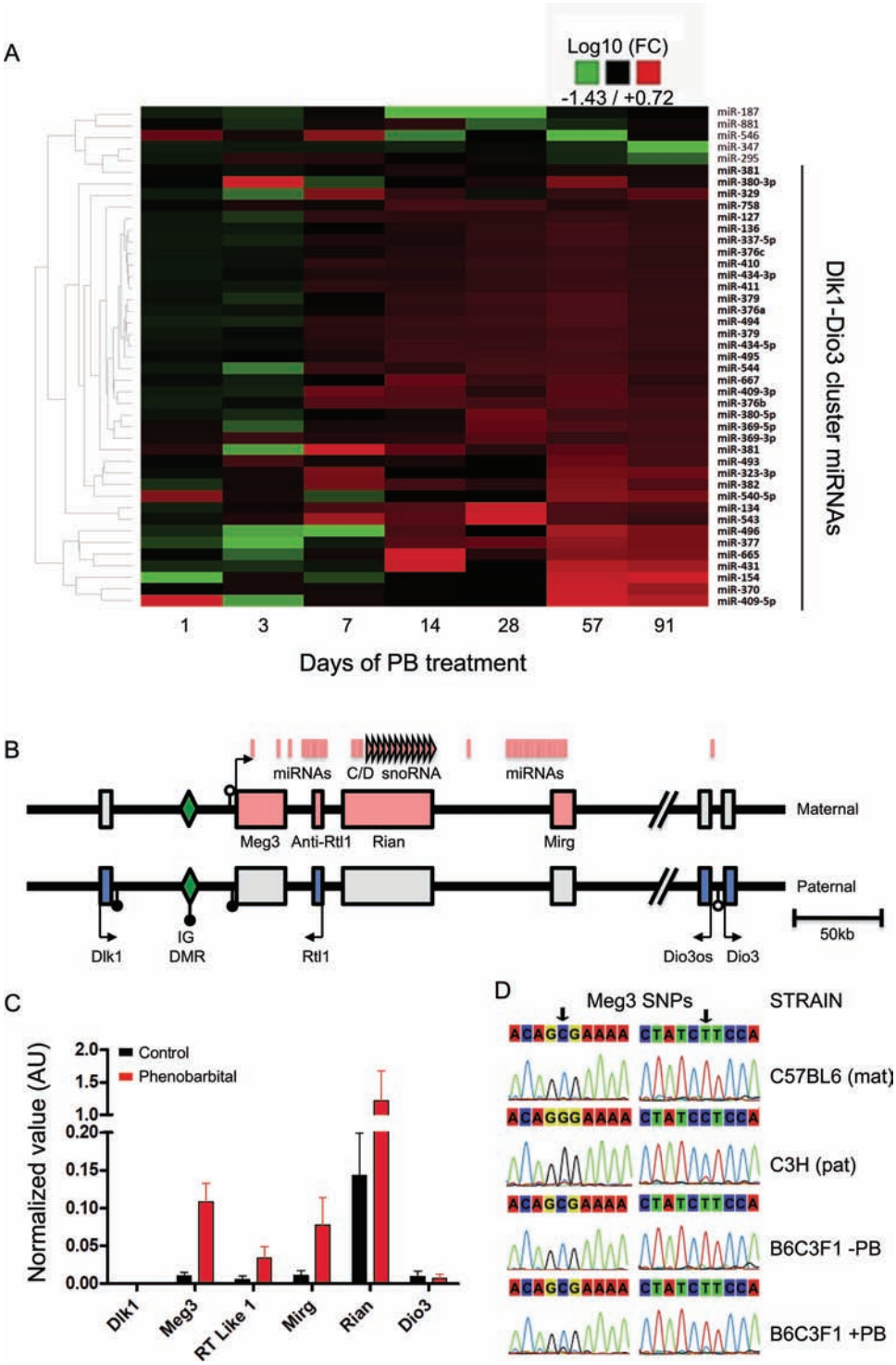

FIG. 3. Kinetic induction of miRNAs and lncRNAs from the *Dlk1-Dio3* imprinted cluster upon PB exposure. (A) miRNA profiling: Expression of 784 miRNAs was measured by using ABI TaqMan miRNA LDA. The heat map shows all the miRNAs that were up- or downregulated more than twofold (with adjusted *p*-value < 0.05) in at least one time point. miRNAs transcribed from the *Dlk1-Dio3* cluster are indicated in bold. (B) Architecture of *Dlk1-Dio3* genomic region: maternal and paternal alleles illustrating the transcripts of parental origin. Under normal conditions, IG-DMR and *Meg3*-DMR methylation of the parental allele regulates the genomic imprinting. (C) PB induction of lncRNAs and *Rtl1* expression from *Dlk1-Dio3* cluster at the 4-week time point. RT-qPCR analysis of lncRNA (*Meg3*, *Rian*, and *Mirg*) and coding gene (*Rtl1*, *Dlk1*, and *Dio3*) expression. (D) Meg3 SNPs electropherograms alignment on liver cDNA from each parental strains (C3H and C57/BL6) and from the 91-day B6C3F1 samples treated (+PB) or untreated (−PB) with PB. Polymorphisms are indicated with arrows, demonstrating maternal expression of the analyzed transcript. A comprehensive allelic analysis is available in Supplementary figure S4A.

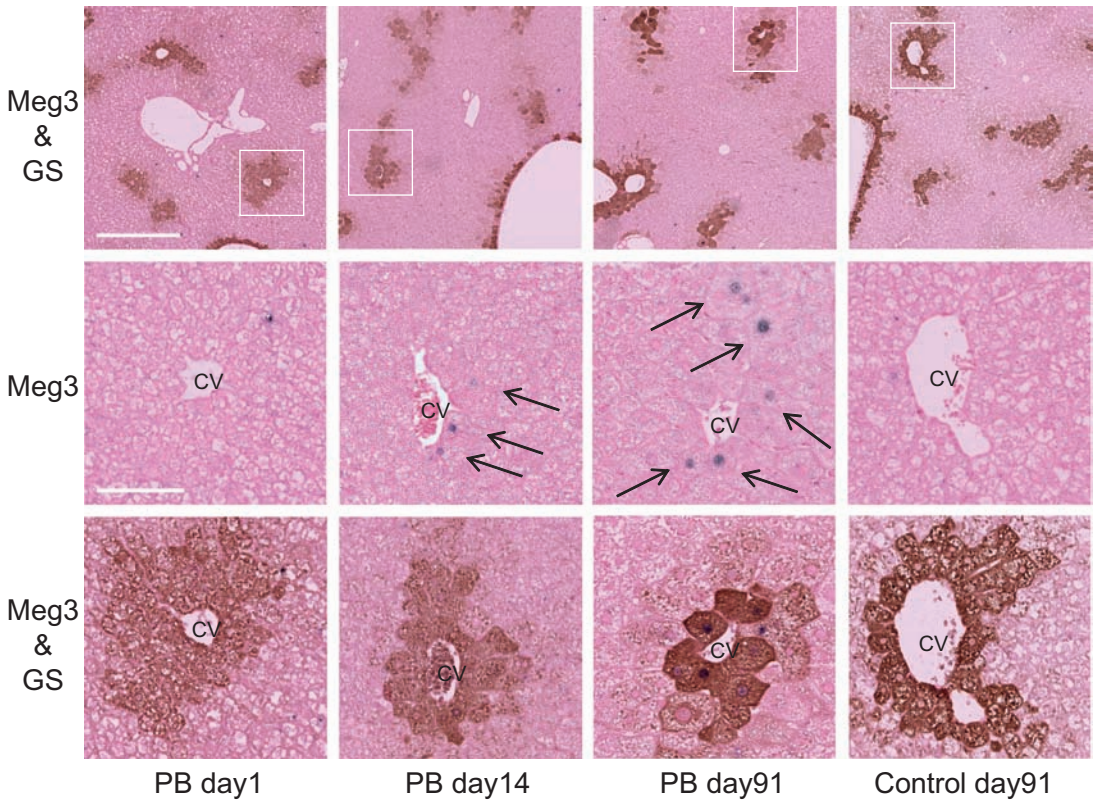

FIG. 4. Expression and localization of *Meg3* in the liver. Upper panel: Colocalization of *Meg3* transcript (ISH: blue) and GS (IHC: brown) protein in control (91 days) and treated (1, 14, and 91 days) livers. Boxes indicate venous regions of the central zone of the lobule that are magnified in the middle and bottom panels. Middle panel: Localization of *Meg3*. Arrows indicate cells showing positive *Meg3* ISH staining. Blue staining at day 1 is unspecific non-nuclear background. Bottom panel: Colocalization of Meg3 and GS stainings. Central vein is indicated by "CV."

2011) that were treated for 12 weeks with either PB or vehicle. PB treatment led to increased *Meg3* and *Rian* transcript levels in C3H WT mouse livers. Basal expression levels of *Meg3* and *Rian* were reduced and induction upon PB treatment was lost in *Ctnnb1*^{KO} mouse livers (Fig. 5A), indicating that β-catenin is required for both the basal expression and PB-induction of the *Dlk1-Dio3* cluster genes. In contrast to CAR^{KO}/PXR^{KO} animals, the *Ctnnb1*^{KO} led to an increase in basal expression levels of *Cyp2b10*, and *Cyp2b10* expression was induced by PB treatment. Together, these results suggest that CAR and β-catenin pathways positively regulate the expression of the *Dlk1-Dio3* cluster lncRNAs (Fig. 5B) and link the regulation of the *Dlk1-Dio3* cluster to the pathways that are essential for tumor promotion by PB.

DISCUSSION

The initiating events and early temporal molecular perturbations leading to NGC are poorly understood. NGC is a common toxicity finding in rodents in preclinical safety assessment, for which no well-validated reliable short-term assays and biomarkers exist. Here, we have used integrated molecular profiling to characterize the temporal dynamics of molecular responses to PB in mouse liver and to identify novel early biomarkers for liver tumor promotion.

We have identified the induction of miRNAs and lncRNAs encoded from the *Dlk1-Dio3* imprinted gene cluster as novel early molecular responses to a liver tumor-promoting dose of PB. The carcinogenic relevance of hepatic *Dlk1-Dio3* cluster ncRNA induction (Fig. 5B) is supported by the following observations: (1) PB induction of *Dlk1-Dio3* cluster ncRNAs is genetically dependent on CAR and β-catenin, two pathways essential for PB-mediated liver tumor promotion; (2) Neither *Meg3* nor *Rian* lncRNAs were upregulated in B6C3F1 mouse kidney following 4 weeks exposure to PB (Lempiainen *et al.*, 2011), consistent with the liver specificity of the carcinogenesis phenotype that is observed following long-term (12 months) PB exposure (Becker, 1982); (3) *Meg3* is overexpressed in PB-promoted liver tumors (Phillips *et al.*, 2009a; Unterberger and Schwarz, unpublished data; Supplementary table); (4) PB induction of the *Dlk1-Dio3* cluster ncRNA expression was reversible, consistent with the observation that NGC tumor promotion effects are usually reversible until a certain point-of-no-return (Spindler *et al.*, 2000). It is also noteworthy that the *Dlk1-Dio3* gene cluster is located close to a genetically characterized mouse *h*epato*c*arcinogenesis *s*usceptibility locus (*hcs3*) on chromosome 12 (Gariboldi *et al.*, 1993).

The molecular functions and targets of the *Dlk1-Dio3* cluster ncRNAs are largely unknown. *Meg3* lncRNA has been reported

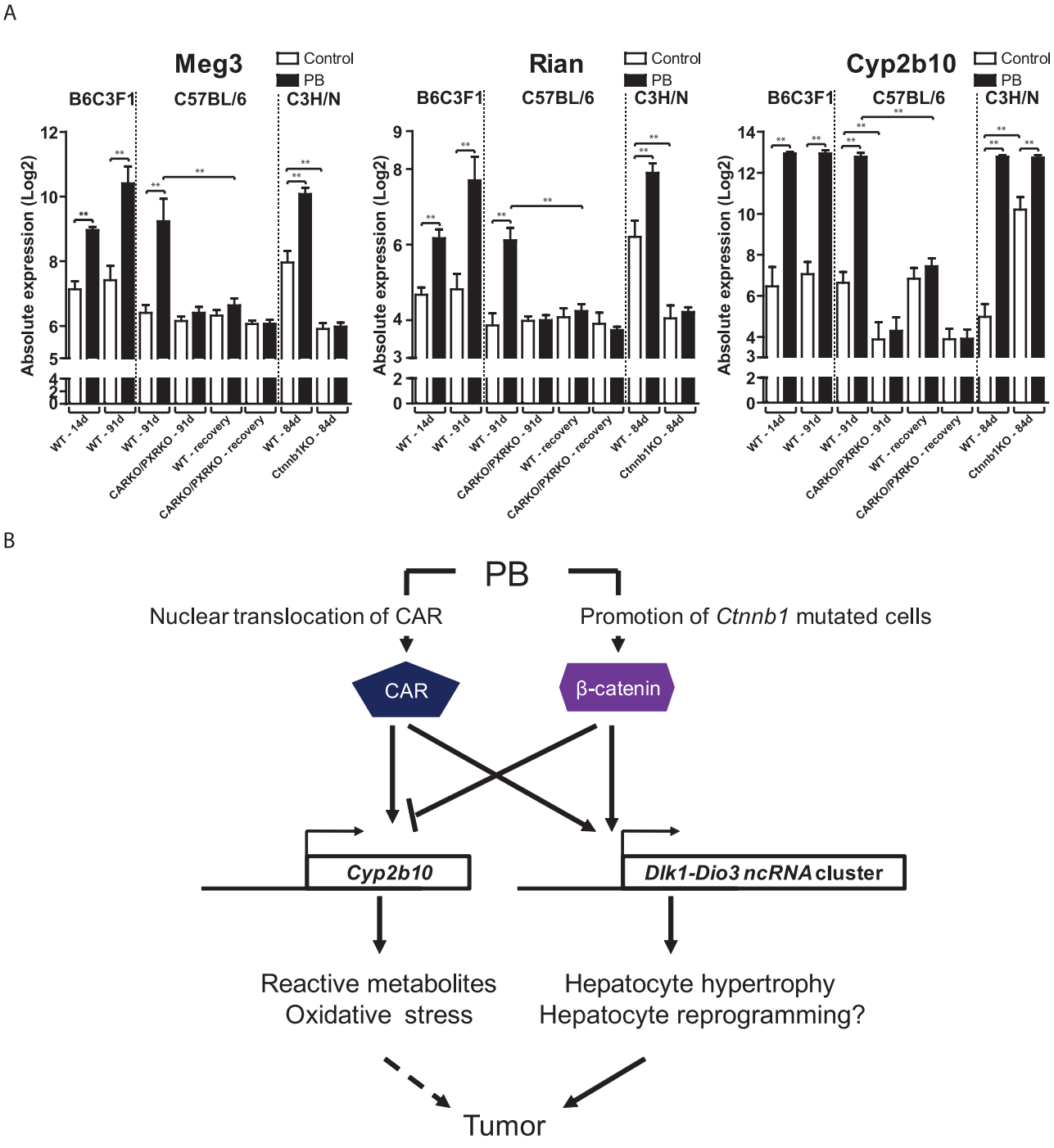

FIG. 5. CAR and beta-catenin pathway dependency, reversibility, and mouse strain differences for *Dlk1-Dio3* cluster lncRNA induction by PB. (**A**) Expression of lncRNAs from the *Dlk1-Dio3* cluster is regulated by CAR/PXR and β-catenin pathways. Expression of *Cyp2b10*, *Meg3*, and *Rian* was determined using Affymetrix GeneChips; bars indicate mean signal values for four to seven biological replicates; lines on top of bars indicate standard deviation. BH statistical analysis was used to calculate significance within the three studies (in different mouse strain backgrounds): *BH < 0.05, fold change > 2; **BH < 0.001, fold change > 2. (**B**) Model for PB-induced perturbation of the *Dlk1-Dio3* cluster ncRNA and *Cyp2b10* expression. PB upregulates the expression of *Dlk1-Dio3* cluster ncRNAs via CAR and β-catenin pathways, whereas *Cyp2b10* expression is induced by CAR pathway but inhibited by β-catenin pathway. The mechanisms by which CAR and β-catenin regulate *Dlk1-Dio3* cluster ncRNAs are currently unknown. The increased expression of *Dlk1-Dio3* ncRNAs upon PB exposure is associated with hepatocyte hypertrophy and, based on literature, might contribute to reprogramming of hepatocytes (Luk *et al.*, 2011). The genetic dependence of *Dlk1-Dio3* cluster ncRNA induction on both CAR and β-catenin supports a role in tumor promotion.

to function as a cofactor of polycomb repressor complex 2, directing the chromatin modifier complex to the *Dlk1* gene and thereby regulating *Dlk1* expression (Zhao *et al.*, 2010). Some of the *Dlk1-Dio3* cluster miRNAs may target *c-Myc* transcripts and thereby regulate cell growth and pluripotency (Thayanithy *et al.*, 2012). An important role for the *Dlk1-Dio3* cluster in regulating cellular stemness is suggested by two publications reporting that *Dlk1-Dio3* transcript levels correlate with pluripotency status of induced pluripotent stem cells (Liu *et al.*, 2010; Stadtfeld *et al.*, 2010). *Dlk1-Dio3* cluster expression perturbations have also been reported in mouse and human hepatocellular carcinomas (HCCs) (Braconi *et al.*, 2011; Luk *et al.*, 2011), and overexpression of these ncRNAs in human HCC samples has been attributed to a subtype of tumors containing stem-like cells that are associated with poor prognosis (Luk *et al.*, 2011). Importantly, the activation of this imprinted domain by *in vivo* gene targeting induces hepatocellular carcinoma, robustly demonstrating a role for the *Dlk1-Dio3* cluster in liver carcinogenesis (Wang *et al.*, 2012). In our study, increased *Meg3* expression upon PB treatment was detected specifically in hypertrophic perivenous hepatocytes. It is not yet clear whether *Meg3* is transcriptionally upregulated by PB in central hepatocytes as part of a hypertrophic response or alternatively whether PB induces the clonal expansion of rare preexisting *Meg3*-expressing hepatocytes in adult liver (hypertrophy/hyperplasia). A possible consequence of *Dlk1-Dio3* cluster ncRNA induction in hypertrophic hepatocytes might be cellular re-programming. There is evidence supporting the dedifferentiation of hepatocytes during hepatocarcinogenesis (Gournay *et al.*, 2002) and both normal and neoplastic non-stem cells can be converted to a stem-like state (Chaffer *et al.*, 2011). The potential role of *Dlk1-Dio3* cluster induction in hepatocyte reprogramming or a "return to stemness" during the early stages of liver tumor promotion thus warrants further investigation.

Our data indicate that *Dlk1-Dio3* cluster ncRNAs might serve as useful early biomarkers of rodent hepatocarcinogenesis. However, an increased understanding of mechanisms underlying carcinogenesis has raised doubts regarding the appropriateness of extrapolating some rodent tumor findings to humans (Holsapple *et al.*, 2006). Prolonged treatment with PB does increase the liver size in humans (Pirttiaho *et al.*, 1982), but human hepatocytes are resistant to the ability of PB to increase cell proliferation (Hasmall and Roberts, 1999; Parzefall *et al.*, 1991) and inhibit apoptosis (Hasmall and Roberts, 1999). There is also a convincing body of epidemiology data indicating that PB is not a human carcinogen (IARC, 2001; Lamminpaa *et al.*, 2002). A human relevance framework concept, with the central tenets being the identification of a mode of action (MoA) and key events, was developed to evaluate human risk based on rodent tumor data, and it has been applied to PB (Holsapple *et al.*, 2006). Increased cell proliferation, hypertrophy, and inhibition of apoptosis are the key CAR-dependent tumorigenic effects of PB (Huang *et al.*, 2005; Wei *et al.*, 2000; Whysner *et al.*, 1996; Yamamoto *et al.*, 2004) and fulfill the criteria for a chemical carcinogenesis MoA (Sonich-Mullin *et al.*, 2001). Cytochrome P450 (Cyp2b10) expression and enzyme activity have recently been proposed as a surrogate biomarker for CAR activation at cessation of a mouse carcinogenesis bioassay (Hoflack *et al.*, 2012). However, cytochrome P450 enzyme activity generally lacks sufficient sensitivity, accuracy, and specificity as an early predictive biomarker for nongenotoxic carcinogens (Elcombe *et al.*, 2002). Although PB-mediated Cyp2b10 induction is dependent on CAR, it can still occur in the absence of β-catenin signaling, thereby unlinking Cyp2b10 regulation from a key signaling pathway required for PB-mediated hepatocarcinogenesis (Rignall *et al.*, 2011). Importantly, we show that PB-mediated *Dlk1-Dio3* cluster ncRNA induction is genetically dependent on both CAR and β-catenin signaling, supporting its candidate biomarker potential. To further evaluate biomarker sensitivity, specificity, and human relevance, it will be important to investigate the expression of the *Dlk1-Dio3* cluster ncRNAs following treatment with a panel of nongenotoxic or genotoxic carcinogens and non-hepatocarcinogens in a range of WT rodent strains and transgenic mouse models expressing the human CAR/PXR nuclear receptors (www.imi-marcar.eu).

SUPPLEMENTARY DATA

Supplementary data are available online at http://toxsci.oxfordjournals.org/.

FUNDING

Innovative Medicine Initiative Joint Undertaking (IMI JU) (115001) (MARCAR project; http://www.imi-marcar.eu/); Novartis; NIBR Postdoctoral Fellowship (to H.L.); IMI-MARCAR funded career development fellowship at the Medical Research Council (MRC) HGU (to J.T., R.M.); IMI-MARCAR (to R.M.); BBC (to R.M.).

ACKNOWLEDGMENTS

All IMI-MARCAR consortium partners had a role in study design, data collection and analysis, decision to publish, or preparation of the manuscript. We thank J.C. Schaffner for pathology analysis and Ernst Gassmann for the LC-MS exposure analyses. Figure 1A was produced using Servier Medical Art (www.servier.com).

REFERENCES

Aydinlik, H., Nguyen, T. D., Moennikes, O., Buchmann, A., and Schwarz, M. (2001). Selective pressure during tumor promotion by phenobarbital leads to clonal outgrowth of beta-catenin-mutated mouse liver tumors. *Oncogene* **20,** 7812–7816.

Bachman, A. N., Phillips, J. M., and Goodman, J. I. (2006). Phenobarbital induces progressive patterns of GC-rich and gene-specific altered DNA methylation in the liver of tumor-prone B6C3F1 mice. *Toxicol. Sci.* **91,** 393–405.

Bartel, D. P. (2004). MicroRNAs: Genomics, biogenesis, mechanism, and function. *Cell* **116,** 281–297.

Becker, F. F. (1982). Morphological classification of mouse liver tumors based on biological characteristics. *Cancer Res.* **42,** 3918–3923.

Benjamini, Y., and Hochberg, Y. (1995). Controlling the false discovery rate: A practical and powerful approach to multiple testing. *J. R. Statist. Soc. B* **57**, 289–300.

Berdasco, M., and Esteller, M. (2010). Aberrant epigenetic landscape in cancer: How cellular identity goes awry. *Dev. Cell* **19,** 698–711.

Bonnet, D., and Dick, J. E. (1997). Human acute myeloid leukemia is organized as a hierarchy that originates from a primitive hematopoietic cell. *Nat. Med.* **3,** 730–737.

Braconi, C., Kogure, T., Valeri, N., Huang, N., Nuovo, G., Costinean, S., Negrini, M., Miotto, E., Croce, C. M., and Patel, T. (2011). microRNA-29 can regulate expression of the long non-coding RNA gene MEG3 in hepatocellular cancer. *Oncogene* **30,** 4750–4756.

Chaffer, C. L., Brueckmann, I., Scheel, C., Kaestli, A. J., Wiggins, P. A., Rodrigues, L. O., Brooks, M., Reinhardt, F., Su, Y., Polyak, K., *et al.* (2011). Normal and neoplastic nonstem cells can spontaneously convert to a stem-like state. *Proc. Natl. Acad. Sci. U.S.A.* **108,** 7950–7955.

Chen, L. L., and Carmichael, G. G. (2010). Decoding the function of nuclear long non-coding RNAs. *Curr. Opin. Cell Biol.* **22,** 357–364.

Counts, J. L., Sarmiento, J. I., Harbison, M. L., Downing, J. C., McClain, R. M., and Goodman, J. L. (1996). Cell proliferation and global methylation status changes in mouse liver after phenobarbital and/or choline-devoid, methionine-deficient diet administration. *Carcinogenesis* **17,** 1251–1257.

Dyer, M. A., and Bremner, R. (2005). The search for the retinoblastoma cell of origin. *Nat. Rev. Cancer* **5,** 91–101.

Elcombe, C. R., Odum, J., Foster, J. R., Stone, S., Hasmall, S., Soames, A. R., Kimber, I., and Ashby, J. (2002). Prediction of rodent nongenotoxic carcinogenesis: Evaluation of biochemical and tissue changes in rodents following exposure to nine nongenotoxic NTP carcinogens. *Environ. Health Perspect.* **110,** 363–375.

Eppig, J. T., Blake, J. A., Bult, C. J., Kadin, J. A., and Richardson, J. E. (2012). The Mouse Genome Database (MGD): Comprehensive resource for genetics and genomics of the laboratory mouse. *Nucleic Acids Res.* **40,** D881–D886.

Esteller, M., and Rodriguez-Paredes, M. (2011). Cancer epigenetics reaches mainstream oncology. *Nat. Med.* **17**, 330–339.

Feinberg, A. P., Ohlsson, R., and Henikoff, S. (2006). The epigenetic progenitor origin of human cancer. *Nat. Rev. Genet.* **7,** 21–33.

Gariboldi M, Manenti G, Canzian F, *et al.* (1993). Chromosome mapping of murine susceptibility loci to liver carcinogenesis. *Cancer Res.* **53,** 209–11.

Gentleman, R. C., Carey, V. J., Bates, D. M., Bolstad, B., Dettling, M., Dudoit, S., Ellis, B., Gautier, L., Ge, Y., Gentry, J., *et al.* (2004). Bioconductor: Open software development for computational biology and bioinformatics. *Genome Biol.* **5,** R80.

Goodman, J. I., and Watson, R. E. (2002). Altered DNA methylation: A secondary mechanism involved in carcinogenesis. *Annu. Rev. Pharmacol. Toxicol.* **42,** 501–525.

Gournay, J., Auvigne, I., Pichard, V., Ligeza, C., Bralet, M. P., and Ferry, N. (2002). In vivo cell lineage analysis during chemical hepatocarcinogenesis in rats using retroviral-mediated gene transfer: Evidence for dedifferentiation of mature hepatocytes. *Lab. Invest.* **82,** 781–788.

Guttman, M., Donaghey, J., Carey, B. W., Garber, M., Grenier, J. K., Munson, G., Young, G., Lucas, A. B., Ach, R., Bruhn, L., *et al.* (2011). lincRNAs act in the circuitry controlling pluripotency and differentiation. *Nature* **477,** 295–300.

Hanahan, D., and Weinberg, R. A. (2011). Hallmarks of cancer: The next generation. *Cell* **144,** 646–674.

Hartmann, M., Roeraade, J., Stoll, D., Templin, M. F., and Joos, T. O. (2009). Protein microarrays for diagnostic assays. *Anal. Bioanal. Chem.* **393,** 1407–1416.

Hasmall, S. C., and Roberts, R. A. (1999). The perturbation of apoptosis and mitosis by drugs and xenobiotics. *Pharmacol. Ther.* **82,** 63–70.

Hoflack, J. C., Mueller, L., Fowler, S., Braendli-Baiocco, A., Flint, N., Kuhlmann, O., Singer, T., and Roth, A. (2012). Monitoring Cyp2b10 mRNA expression at cessation of 2-year carcinogenesis bioassay in mouse liver provides evidence for a carcinogenic mechanism devoid of human relevance: The dalcetrapib experience. *Toxicol. Appl. Pharmacol.* **259,** 355–365.

Holsapple, M. P., Pitot, H. C., Cohen, S. M., Cohen, S. H., Boobis, A. R., Klaunig, J. E., Pastoor, T., Dellarco, V. L., and Dragan, Y. P. (2006). Mode of action in relevance of rodent liver tumors to human cancer risk. *Toxicol. Sci.* **89,** 51–56.

Huang, W., Zhang, J., Washington, M., Liu, J., Parant, J. M., Lozano, G., and Moore, D. D. (2005). Xenobiotic stress induces hepatomegaly and liver tumors via the nuclear receptor constitutive androstane receptor. *Mol. Endocrinol.* **19,** 1646–1653.

IARC. (2001). Phenobarbital and its sodium salt. *IARC Monogr.* **79,** 161–286.

Irizarry, R. A., Hobbs, B., Collin, F., Beazer-Barclay, Y. D., Antonellis, K. J., Scherf, U., and Speed, T. P. (2003). Exploration, normalization, and summaries of high density oligonucleotide array probe level data. *Biostatistics* **4,** 249–264.

Jones, P. A., and Baylin, S. B. (2007). The epigenomics of cancer. *Cell* **128,** 683–692.

Kawamoto, T., Sueyoshi, T., Zelko, I., Moore, R., Washburn, K., and Negishi, M. (1999). Phenobarbital-responsive nuclear translocation of the receptor CAR in induction of the CYP2B gene. *Mol. Cell. Biol.* **19,** 6318–6322.

Keane, T. M., Goodstadt, L., Danecek, P., White, M. A., Wong, K., Yalcin, B., Heger, A., Agam, A., Slater, G., Goodson, M., *et al.* (2011). Mouse genomic variation and its effect on phenotypes and gene regulation. *Nature* **477,** 289–294.

Khalil, A. M., Guttman, M., Huarte, M., Garber, M., Raj, A., Rivea Morales, D., Thomas, K., Presser, A., Bernstein, B. E., van Oudenaarden, A., *et al.* (2009). Many human large intergenic noncoding RNAs associate with chromatin-modifying complexes and affect gene expression. *Proc. Natl. Acad. Sci. U.S.A.* **106,** 11667–11672.

Koerner, M. V., Pauler, F. M., Huang, R., and Barlow, D. P. (2009). The function of non-coding RNAs in genomic imprinting. *Development* **136,** 1771–1783.

Kostka, G., Urbanek, K., and Ludwicki, J. K. (2007). The effect of phenobarbital on the methylation level of the p16 promoter region in rat liver. *Toxicology* **239,** 127–135.

Koturbash, I., Beland, F. A., and Pogribny, I. P. (2011). Role of epigenetic events in chemical carcinogenesis–a justification for incorporating epigenetic evaluations in cancer risk assessment. *Toxicol. Mech. Methods* **21,** 289–297.

Lamminpaa, A., Pukkala, E., Teppo, L., and Neuvonen, P. J. (2002). Cancer incidence among patients using antiepileptic drugs: A long-term follow-up of 28,000 patients. *Eur. J. Clin. Pharmacol.* **58,** 137–141.

LeBaron, M. J., Rasoulpour, R. J., Klapacz, J., Ellis-Hutchings, R. G., Hollnagel, H. M., and Gollapudi, B. B. (2010). Epigenetics and chemical safety assessment. *Mutat. Res.* **705,** 83–95.

Lehmann, J. M., McKee, D. D., Watson, M. A., Willson, T. M., Moore, J. T., and Kliewer, S. A. (1998). The human orphan nuclear receptor PXR is activated by compounds that regulate CYP3A4 gene expression and cause drug interactions. *J. Clin. Invest.* **102,** 1016–1023.

Lempiainen, H., Müller, A., Brasa, S., Teo, S. S., Roloff, T. C., Morawiec, L., Zamurovic, N., Vicart, A., Funhoff, E., Couttet, P., *et al.* (2011). Phenobarbital mediates an epigenetic switch at the constitutive androstane receptor (CAR) target gene Cyp2b10 in the liver of B6C3F1 mice. *PLoS ONE* **6,** e18216.

Liu, L., Luo, G. Z., Yang, W., Zhao, X., Zheng, Q., Lv, Z., Li, W., Wu, H. J., Wang, L., Wang, X. J., *et al.* (2010). Activation of the imprinted Dlk1-Dio3 region correlates with pluripotency levels of mouse stem cells. *J. Biol. Chem.* **285,** 19483–19490.

Loeppen, S., Schneider, D., Gaunitz, F., Gebhardt, R., Kurek, R., Buchmann, A., and Schwarz, M. (2002). Overexpression of glutamine synthetase is associated with beta-catenin-mutations in mouse liver tumors during promotion of hepatocarcinogenesis by phenobarbital. *Cancer Res.* **62,** 5685–5688.

Luk, J. M., Burchard, J., Zhang, C., Liu, A. M., Wong, K. F., Shek, F. H., Lee, N. P., Fan, S. T., Poon, R. T., Ivanovska, I., *et al.* (2011). DLK1-DIO3 genomic imprinted microRNA cluster at 14q32.2 defines a stemlike subtype of hepatocellular carcinoma associated with poor survival. *J. Biol. Chem.* **286,** 30706–30713.

Merlo, L. M., Pepper, J. W., Reid, B. J., and Maley, C. C. (2006). Cancer as an evolutionary and ecological process. *Nat. Rev. Cancer* **6,** 924–935.

Negrini, S., Gorgoulis, V. G., and Halazonetis, T. D. (2010). Genomic instability–an evolving hallmark of cancer. *Nat. Rev. Mol. Cell Biol.* **11,** 220–228.

Parzefall, W., Erber, E., Sedivy, R., and Schulte-Hermann, R. (1991). Testing for induction of DNA synthesis in human hepatocyte primary cultures by rat liver tumor promoters. *Cancer Res.* **51,** 1143–1147.

Phillips, J. M., Burgoon, L. D., and Goodman, J. I. (2009a). The constitutive active/androstane receptor facilitates unique phenobarbital-induced expression changes of genes involved in key pathways in precancerous liver and liver tumors. *Toxicol. Sci.* **110,** 319–333.

Phillips, J. M., Burgoon, L. D., and Goodman, J. I. (2009b). Phenobarbital elicits unique, early changes in the expression of hepatic genes that affect critical pathways in tumor-prone B6C3F1 mice. *Toxicol. Sci.* **109,** 193–205.

Phillips, J. M., and Goodman, J. I. (2008). Identification of genes that may play critical roles in phenobarbital (PB)-induced liver tumorigenesis due to altered DNA methylation. *Toxicol. Sci.* **104,** 86–99.

Phillips, J. M., Yamamoto, Y., Negishi, M., Maronpot, R. R., and Goodman, J. I. (2007). Orphan nuclear receptor constitutive active/androstane receptor-mediated alterations in DNA methylation during phenobarbital promotion of liver tumorigenesis. *Toxicol. Sci.* **96,** 72–82.

Pirttiaho, H. I., Sotaniemi, E. A., Pelkonen, R. O., and Pitkänen, U. (1982). Hepatic blood flow and drug metabolism in patients on enzyme-inducing anticonvulsants. *Eur. J. Clin. Pharmacol.* **22,** 441–445.

Prasanth, K. V., and Spector, D. L. (2007). Eukaryotic regulatory RNAs: An answer to the 'genome complexity' conundrum. *Genes Dev.* **21,** 11–42.

Reya, T., Morrison, S. J., Clarke, M. F., and Weissman, I. L. (2001). Stem cells, cancer, and cancer stem cells. *Nature* **414,** 105–111.

Rignall, B., Braeuning, A., Buchmann, A., and Schwarz, M. (2011). Tumor formation in liver of conditional β-catenin-deficient mice exposed to a diethylnitrosamine/phenobarbital tumor promotion regimen. *Carcinogenesis* **32,** 52–57.

Ross, J., Plummer, S. M., Rode, A., Scheer, N., Bower, C. C., Vogel, O., Henderson, C. J., Wolf, C. R., and Elcombe, C. R. (2010). Human constitutive androstane receptor (CAR) and pregnane X receptor (PXR) support the hypertrophic but not the hyperplastic response to the murine nongenotoxic hepatocarcinogens phenobarbital and chlordane in vivo. *Toxicol. Sci.* **116,** 452–466.

Sato, S., Yoshida, W., Soejima, H., Nakabayashi, K., and Hata, K. (2011). Methylation dynamics of IG-DMR and Gtl2-DMR during murine embryonic and placental development. *Genomics* **98,** 120–127.

Scheer, N., Ross, J., Rode, A., Zevnik, B., Niehaves, S., Faust, N., and Wolf, C. R. (2008). A novel panel of mouse models to evaluate the role of human pregnane X receptor and constitutive androstane receptor in drug response. *J. Clin. Invest.* **118,** 3228–3239.

Smyth, G. K. (2004). Linear models and empirical Bayes methods for assessing differential expression in microarray experiments. *Stat. Appl. Genet. Mol. Biol.* **3,** Article 3.

Smyth, G. K., Ed. (2005). Limma: Linear models for microarray data. In *Bioinformatics and Computational Biology Solutions using R and Bioconductor*, pp. 397–420. Springer, New York.

Sonich-Mullin, C., Fielder, R., Wiltse, J., Baetcke, K., Dempsey, J., Fenner-Crisp, P., Grant, D., Hartley, M., Knaap, A., Kroese, D., *et al.* (2001). IPCS conceptual framework for evaluating a mode of action for chemical carcinogenesis. *Regul. Toxicol. Pharmacol.* **34,** 146–152.

Spindler, P., van der Laan, J. W., Ceuppens, P., Harling, R., Ettlin, R., and Lima, B. S. (2000). Carcinogenicity testing of pharmaceuticals in the European Union: A workshop report. *Drug Inf. J.* **34**: 821–828.

Stadtfeld, M., Apostolou, E., Akutsu, H., Fukuda, A., Follett, P., Natesan, S., Kono, T., Shioda, T., and Hochedlinger, K. (2010). Aberrant silencing of imprinted genes on chromosome 12qF1 in mouse induced pluripotent stem cells. *Nature* **465,** 175–181.

Thayanithy, V., Sarver, A. L., Kartha, R. V., Li, L., Angstadt, A. Y., Breen, M., Steer, C. J., Modiano, J. F., and Subramanian, S. (2012). Perturbation of 14q32 miRNAs-cMYC gene network in osteosarcoma. *Bone* **50,** 171–181.

Thomson, J. P., Lempiäinen, H., Hackett, J. A., Nestor, C. E., Müller, A., Bolognani, F., Oakeley, E. J., Schübeler, D., Terranova, R., Reinhardt, D., *et al.* (2012). Non-genotoxic carcinogen exposure induces defined changes in the 5-hydroxymethylome. *Genome Biol.* **13,** R93.

Tolson, A. H., and Wang, H. (2010). Regulation of drug-metabolizing enzymes by xenobiotic receptors: PXR and CAR. *Adv. Drug Deliv. Rev.* **62,** 1238–1249.

Wang, P. R., Xu, M., Toffanin, S., Li, Y., Llovet, J. M., and Russell, D. W. (2012). Induction of hepatocellular carcinoma by in vivo gene targeting. *Proc. Natl. Acad. Sci. U.S.A.* **109,** 11264–11269.

Wei, P., Zhang, J., Egan-Hafley, M., Liang, S., and Moore, D. D. (2000). The nuclear receptor CAR mediates specific xenobiotic induction of drug metabolism. *Nature* **407,** 920–923.

Whysner, J., Ross, P. M., and Williams, G. M. (1996). Phenobarbital mechanistic data and risk assessment: Enzyme induction, enhanced cell proliferation, and tumor promotion. *Pharmacol. Ther.* **71,** 153–191.

Wrzodek, C., Schröder, A., Dräger, A., Wanke, D., Berendzen, K. W., Kronfeld, M., Harter, K., and Zell, A. (2010). ModuleMaster: A new tool to decipher transcriptional regulatory networks. *BioSystems* **99,** 79–81.

Xie, W., Barr, C. L., Kim, A., Yue, F., Lee, A. Y., Eubanks, J., Dempster, E. L., and Ren, B. (2012). Base-resolution analyses of sequence and parent-of-origin dependent DNA methylation in the mouse genome. *Cell* **148,** 816–831.

Yamamoto, Y., Moore, R., Goldsworthy, T. L., Negishi, M., and Maronpot, R. R. (2004). The orphan nuclear receptor constitutive active/androstane receptor is essential for liver tumor promotion by phenobarbital in mice. *Cancer Res.* **64,** 7197–7200.

Zhao, J., Ohsumi, T. K., Kung, J. T., Ogawa, Y., Grau, D. J., Sarma, K., Song, J. J., Kingston, R. E., Borowsky, M., and Lee, J. T. (2010). Genome-wide identification of polycomb-associated RNAs by RIP-seq. *Mol. Cell* **40,** 939–953.